Chondrites and the Protoplanetary Disk
ASP Conference Series, Vol. 341, 2005
A. N. Krot, E. R. D. Scott, & B. Reipurth, eds.

Experimental Constraints on Chondrule Formation

R. H. Hewins

CP 52 LEME, Muséum National d'Histoire Naturelle, 57 rue Cuvier, 75321 Paris CEDEX 05, France

Laboratoire Magmas et Volcans,OPGC - Université Blaise Pascal, 5 rue Kessler, 63038 Clermont-Ferrand cedex, France

Geological Sciences, Rutgers University, 610 Taylor Road, Piscataway, NJ 08854, USA

H. C. Connolly, Jr.

Physical Sciences, Kingsborough College and the Graduate School of the City University of New York, 2001 Oriental Blvd., Brooklyn, NY 10024, USA

Earth and Planetary Sciences, American Museum of Natural History, Central Park West, New York, NY 11024, USA

G. E. Lofgren

Astromaterials Acquisition and Curation, NASA Johnson Space Center, Houston, TX 77058, USA

G. Libourel

Centre de Recherches Pétrographiques et Géochimiques, CRPG-CNRS, UPR 2300, 15 Rue Notre-Dame des Pauvres, BP 20, 54501 Vandoeuvre les Nancy, France

Ecole Nationale Supérieure de Géologie, ENSG-INPL, BP40, 54501 Vandoeuvre-les-Nancy, France

Abstract. Chondrule textures depend on the extent of melting of the chondrule precursor material when cooling starts. If viable nuclei remain in the melt, crystallization begins immediately, producing crystals with shapes that approach equilibrium. If not, crystallization does not occur until the melt is supersaturated, resulting in more rapid growth rates and the formation of skeletal or dendritic crystals. A chondrule texture thus indicates whether nuclei were destroyed, which implies a melting temperature above the liquidus temperature for its particular composition. The presence or absence of skeletal or dendritic crystals in chondrules can be used to constrain their peak temperatures, which range from 1400-1850ºC. Heating times of less than a second result in aggregates of starting materials coated with glass, resembling agglutinates rather than objects with typical chondrule textures, suggesting that heating times are longer. Chondrule textures can be duplicated with a very wide range of cooling rates, but if olivine zoning is to be matched the cooling rate should be within the range 10-1000°C/hr. The size of overgrowths on relict grains cannot be used to infer cooling rates. Chondrules melted in a canonical nebular gas lose sulfur and alkalis in minutes, while iron loss from the silicate melt continues over many hours. Mass loss and isotopic fractionation can be suppressed if the partial pressures of the species of interest are high enough in the ambient gas. Chondrule bulk and mineral composition arrays can be reproduced to a large extent by evaporation. However, condensation of SiO into the melt can simulate the zonation in some chondrules, with pyroxene and a silica polymorph near the rims. The partial equilibration of chondrule melt with non-canonical nebular gas would require heating for time periods of hours.

1. General Introduction

Chondrules, tiny spherules containing olivine, pyroxene, metal, sulfide and glass, with igneous textures, are the most abundant components in most chondritic meteorites, accounting for up to 80% of the rock (e.g., Zanda 2004; Jones et al. this volume). Chondritic bodies are in turn abundant throughout the main asteroid belt. Chondrules therefore document widespread heating in the early inner solar system. The central question of whether the heating mechanism was an astrophysical process or a planetary process is still not totally resolved, though heating by shock waves in the protoplanetary disk (e.g., Desch & Connolly 2002; Desch et al. this volume) is currently one of the most favored mechanisms.

Chondrules might have been formed by condensation of gas (Varela et al. 2002), by agglomeration of a mist of microdroplets and dust (Wood 1996), or by melting of rock or of dustballs (e.g., Jones et al. this volume). There is evidence for formation of small cryptocrystalline chondrules in CB and CH chondrites by direct condensation of liquids (Krot et al. 2001), and of condensation of SiO into Mg-rich chondrule melts (Krot et al. 2003; Libourel et al. 2003). In the case of formation of chondrules from solids, the precursors are widely assumed to be nebular condensates, i.e. fine-grained mineral dust, either of fractionated or of CI composition, though such material cannot easily be converted into typical chondrules (e.g., Hewins & Fox 2004; Jones et al. this volume). Some larger grains were probably present, either relicts of fragmented chondrules of different composition or of annealed condensates or refrac-

tory inclusions (Jones 1996a; Jones et al. 2004; Yurimoto & Wasson 2002). The dispersion of oxygen isotopic compositions of olivine and bulk chondrule suggests a history of exchange of primitive material with nebular gas.

Chondrules have a wide range of bulk compositions, inherited from precursors or explicable by evaporation and condensation, and a spectrum of textures controlled by the nature of their precursors and their thermal histories (e.g., Grossman 1988; Sears 1996; Hewins 1997; Connolly & Desch 2004; Zanda 2004; Jones et al. this volume). Since experimental petrology cannot be used to constrain the origins of chondrules, unless this diversity is considered, we here briefly define the key terms and concepts used in describing them.

Chondrule compositional and textural types are described in McSween (1977), Scott & Taylor (1983), Jones (1996b, and references therein), Hewins (1997), Hewins et al. (1997) and Jones et al. (this volume). Chondrule classification based on their work is as follows. Type I are FeO-poor (unless metamorphosed) and Fe-metal-bearing, and type II are FeO-rich. Type I chondrules are dominant in carbonaceous chondrites and type II chondrules are dominant in ordinary chondrites (McSween 1977; Zanda 2004). Each type is subdivided into A, AB and B according to the olivine/pyroxene ratio (Scott & Taylor 1983), which depends on SiO_2 content and thermal history. The textures are indicated by abbreviations such as P porphyritic, MP microporphyritic, B barred and R radiating, coupled with O and P at the end for olivine and pyroxene. Thus IA MPO, IAB POP, and IIB RP constitute fairly complete descriptions of chondrules (Hewins 1997). Chondrule textures are illustrated in Figures 1 and 2.

Porphyritic olivine chondrules vary considerably in grain size, with type IIA generally being porphyritic, but type IA generally microporphyritic. Even finer-grained chondrules have been described variously as dark-zoned, granular and agglomeratic (Weisberg & Prinz 1996). Such chondrules can be seen in backscattered electron (BSE) images to be porphyritic on a very fine scale, or cryptoporphyritic, or else porphyritic only in patches interstitial to relict material (protoporphyritic). Crystal number densities yield nominal grain sizes of 100, 40, 10 and 5 μm as the transitions between BO, PO, MPO, cryptoporphyritic and protoporphyritic textures (Hewins et al. 1997; Hewins & Fox 2004).

Experiments aimed at producing chondrule-like objects in the laboratory have a history of over thirty years (e.g., Nelson et al. 1972). They have moved from simply producing melt droplets, and then crystallizing them, to exploring melt-solid and melt-gas interaction. Given the great diversity of chondrules, laboratory experiments are invaluable in yielding information on chondrule formation process(es) and for deciphering their initial conditions of formation together with their thermal history. In addition, they provide some critical parameters for astrophysical models of the solar system and of nebular disk evolution in particular (partial pressures, temperature, time, opacity, etc). The early work is best summed up in Lofgren (1996), where the key role of melting history and heterogeneous nucleation in controlling chondrule textures is emphasized. In this paper, we aim particularly at integrating the results of chondrule simulation experiments performed since Lofgren (1996) into the existing framework of chondrule studies. We also concentrate our attention on the formation of chondrules with porphyritic textures, because these are the most abundant.

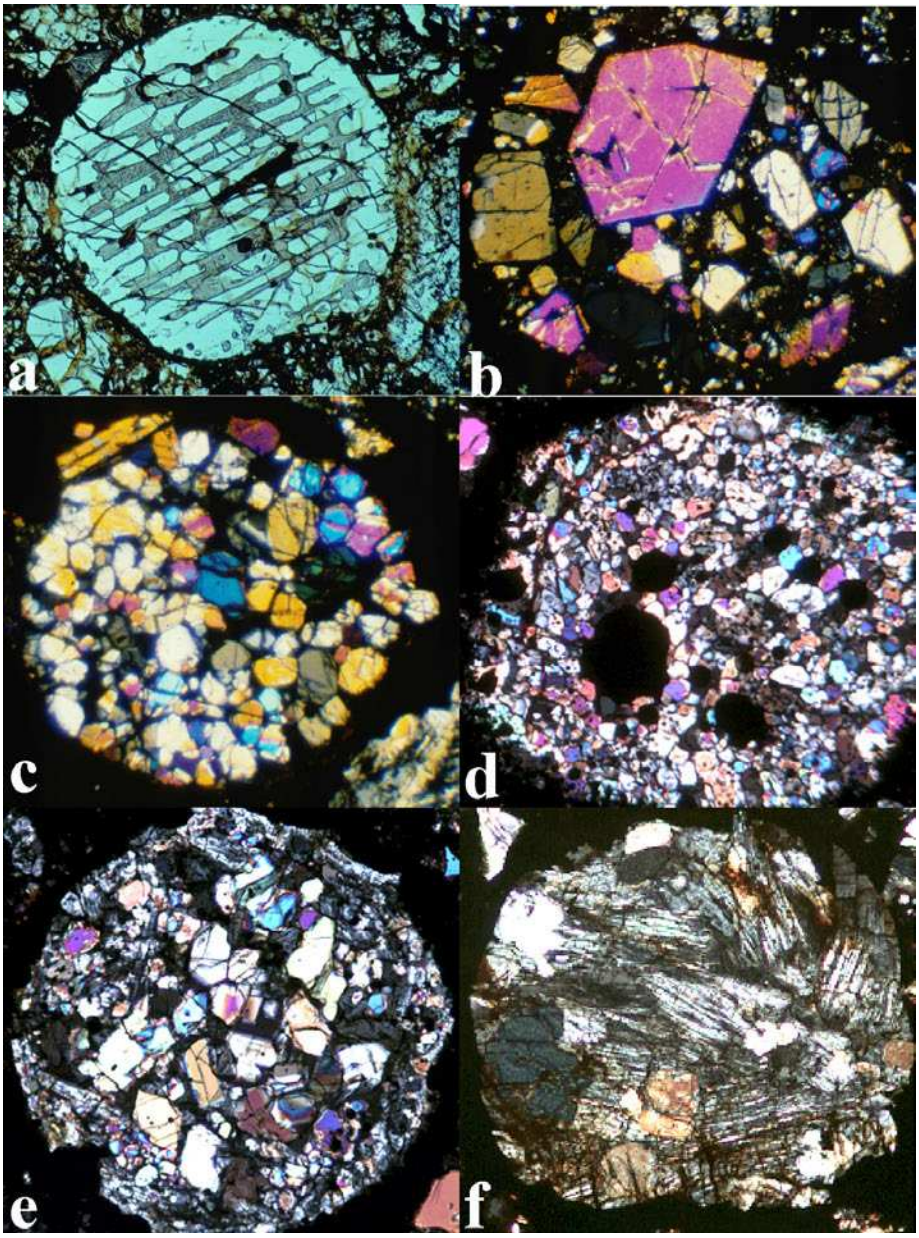

Figure 1. Olivine- and pyroxene-rich chondrules. (a) Barred olivine chondrule, PPL, olivine light grey, glass medium grey. (b) Type IIA PO chondrule, XPL, euhedral olivine phenocrysts in glass (black). (c) Metal-rich type IA MPO chondrule, XPL, olivine white and grey, metal black. (d) Type IA MPO chondrule, XPL. (e) Type IA POP, XPL, olivine white and grey in center, pyroxene grey near margin. (f) Type I(A)B P(O)P, XPL, olivine grey and white, pyroxene showing twinning. PPL = plane polarized light; XPL = cross polarized light. Average diameter ~700 μm. (c) – (f) courtesy of B. Zanda.

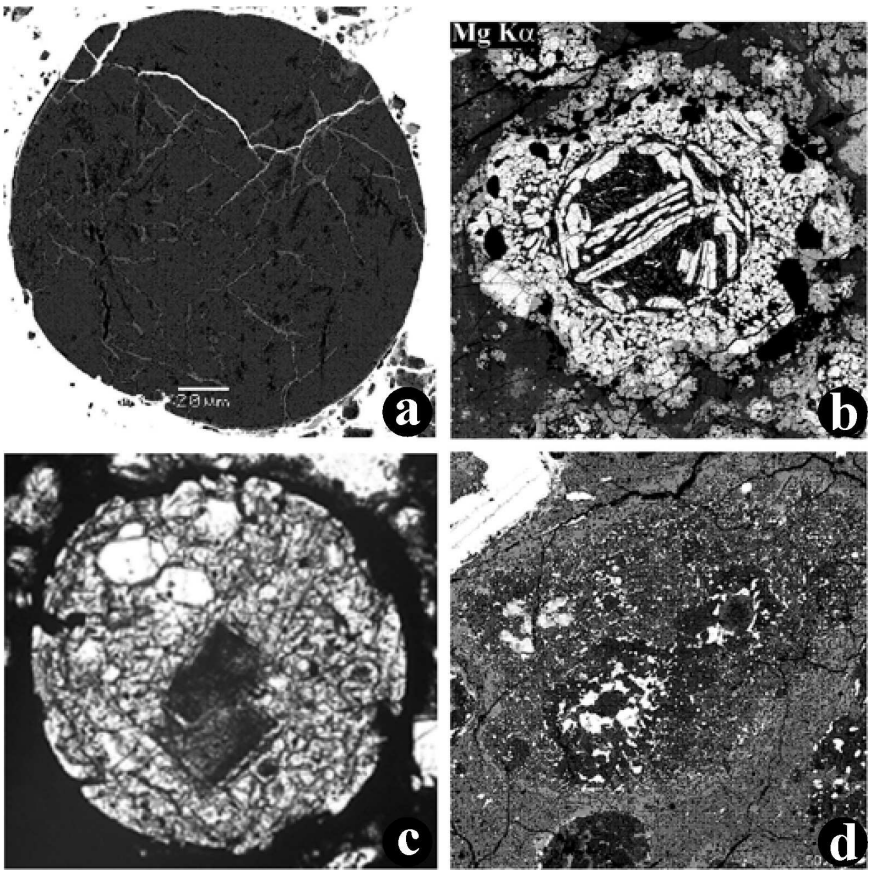

Figure 2. (a) Cryptocrystalline chondrule from the CB chondrite Hammadah al Hamra 237, BSE. (b) 500-μm thick igneous rim on 1 mm BO/PO chondrule in the CV chondrite Efremovka, Mg X-ray image. (c) 750-μm diameter Type IAB chondrule in Chainpur with dusty olivine relict grains, PPL. (d) Chondrule in the CR chondrite Renazzo 1.5 mm long consisting of an aggregate of coarser grained and finer grained domains, BSE, olivine black, metal white. PPL = ordinary light, BSE = back-scattered electrons. (a) and (b) courtesy of A. Krot.

Ideally, by comparing the charges prepared in these experiments with natural chondrules, we can define the peak temperature, heating time and cooling rate experienced by most chondrules. However, there are many complications in inferring the formation conditions of chondrules: there may be several thermal histories that produce similar textures; differences in precursor properties may influence chondrules; chondrule melts may collide with dust grains, or experience evaporation and/or condensation. Chondrule properties are intimately related to the pair of parameters peak temperature and duration of the heating pulse. In particular, long heating time and high peak temperature both contribute to dissolution of crystals and the elimination of nuclei, meaning that it is difficult to define either heating time or peak

temperature uniquely. Recent experiments also demonstrate effects due to evaporation or condensation during melting and solidification, and mixing of objects during the heating process. However, note again that the results for each set of experiments need not be definitive for natural chondrules. They give formation conditions for chondrules only as formed by a chosen chondrule model, e.g., partial melting of coarse solid precursors, dust seeding of total melts, condensation, etc., for the particular physical conditions (including gas compositions and pressures) of the experiments.

2. Texture Simulation Experiments and Thermal History

Most of the experiments simulating chondrules have been based on the assumption that they formed by melting of an aggregate of solid grains, with total pressure in their formation environment of little importance in producing textures, and that they experienced virtually no gain or loss of elements from or to the ambient nebular environment. Typically experiments used pressed pellets attached to Pt wires, heated at 1 atm pressure, but we also discuss here experiments in which small quantities of solids injected into the furnace were incorporated into a droplet or large amounts agglomerated together during the course of cooling. The oxidation state of the charges was controlled by gas mixing. [The oxygen fugacity (fO_2) of an experiment is given in terms of $\log(fO_2)$ relative to the iron-wustite (IW) buffer curve, a temperature dependent parameter that defines equilibrium between Fe^0 and Fe^{2+}. Therefore "IW-1" means that the oxygen fugacity is one log unit below the IW buffer at the temperature given.] Loss of alkali elements by evaporation and Fe to the support wire were significant in many cases. Although the experimental charges were not closed systems, this has no obvious effect on textures, and the results have been applied to the closed system model of chondrule formation. However, Fe loss can influence olivine zoning and thus complicate interpretation of cooling rates (Weinbruch et al. 1998). Experiments specifically designed to study interactions between the chondrule melt and a gas phase are discussed in section 3.

2.1. Textures

The hierarchy of crystal morphologies with respect to extent of melting has been well established, as well as the importance of heterogeneous nucleation (e.g., Lofgren & Russell 1986; Lofgren 1989, 1996; Radomsky & Hewins 1990; Faure et al. 2003). A silicate liquid which is totally melted and superheated (heated above its liquidus temperature, or temperature above which at equilibrium no crystals are present) contains some memory of crystalline material in the form of embryos, which may graduate to viable nuclei a long way below the liquidus temperature during cooling, unless this is so fast that a glass is formed. The ensuing crystal growth is rapid because the supercooled liquid is far from equilibrium (supersaturated), and therefore the crystals are skeletal, dendritic or spherulitic as the growth rate of the crystals increases with the degree of supercooling (Lofgren 1996). Alternatively, a melt may contain relict grains or viable nuclei on which growth can commence immediately when heating and dissolution stop, giving rise to crystals that have equilibrium shapes and for most phases are equant. The size of the crystals depends on the number density of nuclei or relict grains. The sequence of textures in chondrules depends on the temperature and

duration of melting and for many chondrule formation mechanisms it is easier to envisage large variations in temperature than in heating time. There is considerable potential in the use of crystal size distribution (CSD) analysis of charges and chondrules for deciphering chondrule formation conditions (Zieg & Lofgren 2002, 2003).

The abundance of grains that are relicts of the starting material and not crystallized from the melt gives a minimum estimate of the extent of melting, given that some relict material may not be recognizable. Growth on existing grains with little supercooling is the dominant process for most PO textures, whereas for some PO and for BO chondrules the textures form as the result of rapid growth caused by heterogeneous nucleation at high degrees of supercooling. In most PO charges, olivine growth begins when cooling begins and continues until quenching. Relatively precise growth rates can be estimated in charges with obvious relict grains, and they are influenced by both precursor grain size and extent of melting. In the experiments of Hewins & Fox (2004), all made with a cooling curve approximating 800°C/hr, olivine growth rates range from about 1 μm/hr for the finest starting materials with a peak temperature of 1470°C to about 50 μm/hr for the coarsest starting materials heated to 1550°C. For higher temperatures, relicts are no longer obvious, skeletal crystals indicate commencement of growth some unknown time after the onset of cooling, and anisotropy becomes important. For the same compositions and cooling curve (Hewins & Fox 2004), for BO produced with peak temperatures near 1600°C, maximum growth rates are in excess of 7000 μm/hr.

The simulation of chondrules with non-porphyritic textures has been reviewed in earlier papers (Hewins 1988; Lofgren 1996), to which little need be added. There are, however, new contributions (Faure et al. 2003; Tsuchiyama et al. 2004) relevant to the formation of BO chondrules (Fig. 3). Faure et al. (2003) discussed the nature of the transition from skeletal hopper phenocrysts to a dendritic swallowtail morphology, as a function of increased supercooling. Barred or parallel plate olivine develops by preferential growth of dendrites from the external corners of hoppers, and is favored by gradients in temperature or composition. Nagahara & Ozawa (1996) produced BO textures by isothermal evaporation above the original liquidus temperature but *below* the final liquidus temperature. Tsuchiyama et al. (2004) demonstrated that the "bars" were indeed parallel plate crystals by means of x-ray computed tomography. Their experiments were conducted in vacuum and the best matches to classic BO chondrule textures complete with rims were developed in charges with high peak temperatures (100°C or more above the liquidus) and heating times 10-60 minutes. With lower peak temperatures, the charges tended to be spherulitic and lacked rims. Tsuchiyama et al. (2004) emphasize that the precise textures of BO chondrules, with solid rather than skeletal or dendritic bars, have never been reproduced, and annealing after crystallization (a few days at 1200°C) would be required to generate them. This is consistent with the very low cooling rates indicated by subsolidus changes in chondrules (Weinbruch et al. 2001). Excentroradial and barred textures have been formed instead of glass when highly supercooled total melts were impacted by one or several mineral dust grains which acted as seeds (Connolly & Hewins 1995).

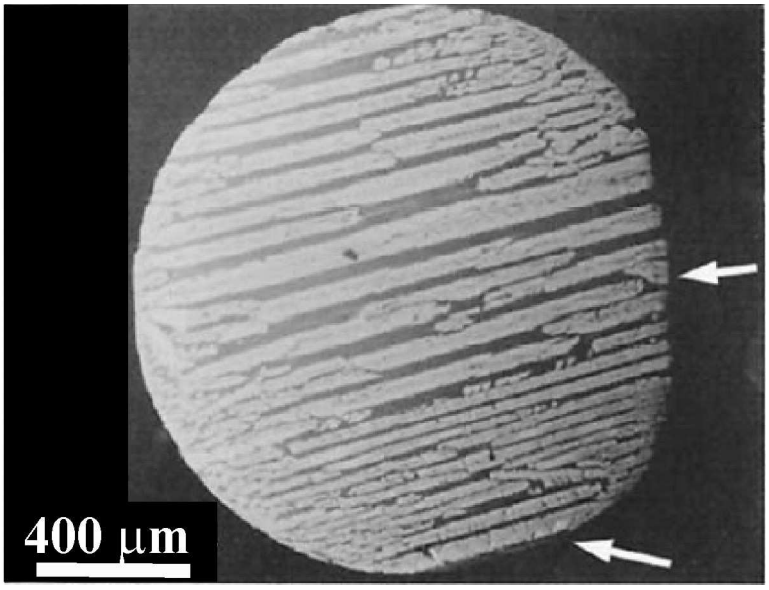

Figure 3. Barred olivine charge made by heating a highly ferroan composition in vacuum 183°C above its liquidus for ten minutes before cooling at 1000°C/hr (Tsuchiyama et al. 2004). Arrows indicate flat surfaces in contact with the graphite crucible.

In recent years, experiments have been designed to investigate the difference in grain sizes of PO (Connolly et al. 1998; Hewins & Fox 2004) and the effects of low degrees of melting (Lofgren et al. 1999; Lofgren & Le 2000; Lofgren & Le 2002; Nettles et al. 2003). Connolly et al. (1998) and Hewins & Fox (2004) examined chondrule textures as a function of precursor grain size, using a total size range of starting material from 125-250 to 1-3 μm. Very fine-grained textures (3-5 μm), such as those of dark-zoned or protoporphyritic chondrules, could be made only if the precursors are equally fine-grained. Such textures are obtained over a wide range of peak temperatures, as long as the peak temperature is below the liquidus, as higher degrees of melting tend to reduce the size of all the precursor grains, without reducing their number much. Only very close to the liquidus is the number of relicts and nuclei drastically reduced so that large crystals can grow during cooling, and the ensuing texture can reasonably be called porphyritic. In contrast, for experiments using coarser-grained starting materials (about 40 μm and above), and any peak temperature below the liquidus, the textures are broadly porphyritic. Figure 4 shows that similar porphyritic textures are obtained from starting materials of different grain size only for peak temperatures near the liquidus and that otherwise the memory of the starting material is obvious.

Lofgren et al. (1999), Lofgren & Le (2000) and Nettles et al. (2003) showed that the textures of some porphyritic chondrules with relict grains in ordinary chondrites can be duplicated by partial melting of crushed unequilibrated ordinary chondrite. Starting material with grain sizes of 1-100 μm produces many large angular relict

grains accompanied by finer (~5 μm) phenocrysts that grew during the experiment. These charges resemble what Hewins et al. (1997) called protoporphyritic chondrules. The higher the degree of melting, the more closely the texture resembles porphyritic textures lacking obvious relict grains. With as little as 50% melting, the porphyritic textures are similar to those produced from a total melt (Fig. 5).

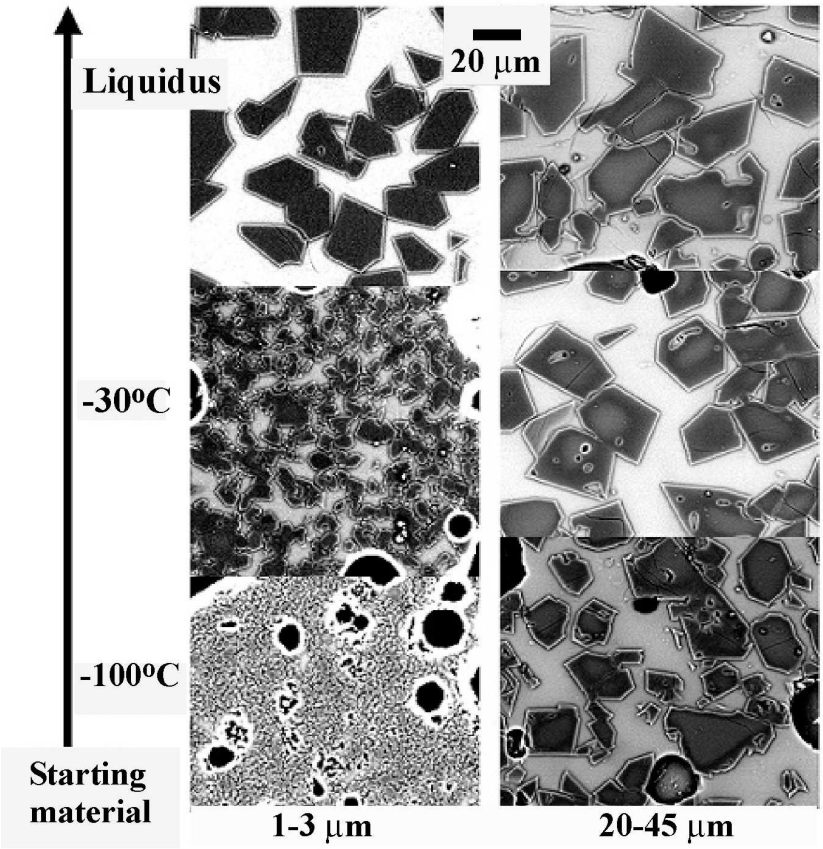

Figure 4. The grain size of a porphyritic charge of type IA/IAB composition depends to a large extent on the grain size of the starting material, except when maximum temperatures approach the liquidus (Hewins & Fox 2004). Heated for 1 min at peak temperature at IW-0.5 and cooled at an average of 800ºC/hr.

Chondrules with many relict grains might be made exclusively or dominantly from recycled chondrule material, whereas the very fine-grained precursor of dark-zoned chondrules is a good candidate for nebular condensate. Nebular condensates are expected to be very fine-grained (e.g., Grossman 1988). The whole range of chondrule textures could not be generated from very fine-grained material in a single rapid melting event, because melting fine-grained material (1-3 μm) produces

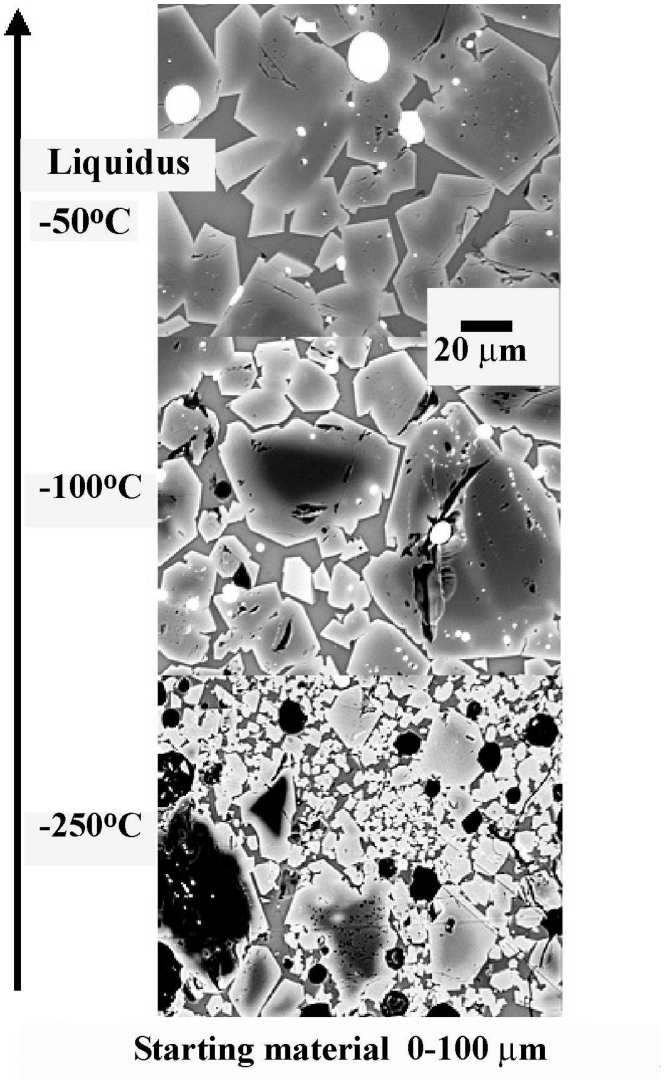

Figure 5. When the starting material is very heterogeneous in grain size, the resulting charges are porphyritic, with relict grains disappearing and olivine sizes becoming more homogeneous for higher peak temperatures. Crushed ordinary chondrite melted for 5 min at IW-3.5 and cooled at 1000ºC/hr (Lofgren & Le 2000).

dominantly fine-grained (5-8 μm) textures (Hewins & Fox 2004). Yu & Hewins (1998) investigated whether repeated heating and cooling of the same charge could lead to coarsening of porphyritic textures. They found that multiple (thirty) heating events with the same peak heating temperature do not lead to significant change in grain size (Yu & Hewins 1998). However, Fox & Hewins (2005) found that, when the second heating is to a higher temperature than the first (and the charge is not to-

tally melted), coarsening of a microporphyritic charge occurs on second cooling. Reducing the numbers of seeds by dissolution, either by longer heating or by reheating events, generates coarser textures on cooling, up to the point where no nuclei can be reformed, resulting in a glass. Fox & Hewins (2005) listed reheating of fine-grained chondrules as one of several ways fine-grained condensate material could be converted to typical porphyritic chondrules. Other explanations of the dominance of porphyritic textures in chondrules include prolonged heating of fine-grained material in a single event, which allows coarsening of relict grains to produce porphyritic texture (Cohen et al. 2000, 2004), and a single heating of coarse-grained precursors, which produces porphyritic textures for a wide range of peak temperatures (Lofgren & Le 2000; Hewins & Fox 2004).

While incomplete melting of solid aggregates is the most accepted origin for porphyritic chondrules, especially in view of relict grains, it is not the only way they might have formed. Connolly & Hewins (1995) examined what happened when totally melted charges, which would have formed glass if cooled in isolation, collided with mineral dust grains (olivine, pyroxene, corundum, diamond or SiC) injected into the furnace. Pristine chondrite matrix, IDPs and comets all contain grains of olivine, pyroxene and amorphous silicate (Scott & Krot 2005), as well as presolar grains, which could conceivably have interacted with chondrules. Such grains were probably processed during chondrule formation (Desch & Connolly 2002; Scott & Taylor 2005), and the largest and most refractory could have collided with molten droplets. A great variety of textures was produced by Connolly & Hewins (1995), depending on the degree of supercooling of the liquid when the dust was puffed and the quantity of dust puffed, i.e. the number of crystal growth sites introduced into the liquid, but independent of the particular mineral puffed. However, in a silica-rich IIAB composition, pyroxene nucleated more frequently on pyroxene seeds and olivine on olivine seeds. Porphyritic textures were produced for small degrees of supercooling and large quantities of dust; radiating and barred textures were formed for greater supercooling and less dust, consistent with more rapid growth. Chondrules formed by collisions with dust grains would contain xenocrysts that acted as seeds, which might be mistaken for relict grains (Fig. 6). Such seeds grow very thin rims while the normal size crystals grow from the melt (Fig. 6).

Wood (1996) proposed that chondrules formed by the agglomeration of a mist of microdroplets and grains, rather than by heating of an aggregate. Yu et al. (1998) achieved the growth of chondrule-like objects without a precursor aggregate or melt droplet, by puffing mineral dust into a furnace at 1600ºC for 30 min at IW-0.5 with Pt wire as a target. Pyroxene and plagioclase from Stillwater norite formed microdroplets of melt, while more refractory San Carlos olivine survived at least in part. Droplets were caught and grown on Pt wire, generally coalescing over time into larger objects. Puffing was resumed at 1400ºC. On cooling, porphyritic textures were formed for $Ol_{20}Nor_{80}$ mixtures, with multiple coarse-grained cores and finer grained mantles (Fig. 7a). These globules resembled some layered and composite chondrules found particularly in CR chondrites. For a more refractory $Ol_{50}Nor_{50}$ mixture, partial dissolution of the olivine resulted in strong reverse zoning, and discontinuous puffing during cooling resulted in finer-grained igneous rims formed on droplets (Fig. 7b). Thus, a single cooling event in which a mist of droplets and grains accreted into a

spherule produces a rimmed object (Yu et al. 1998) resembling those for which two separate heating events have been proposed.

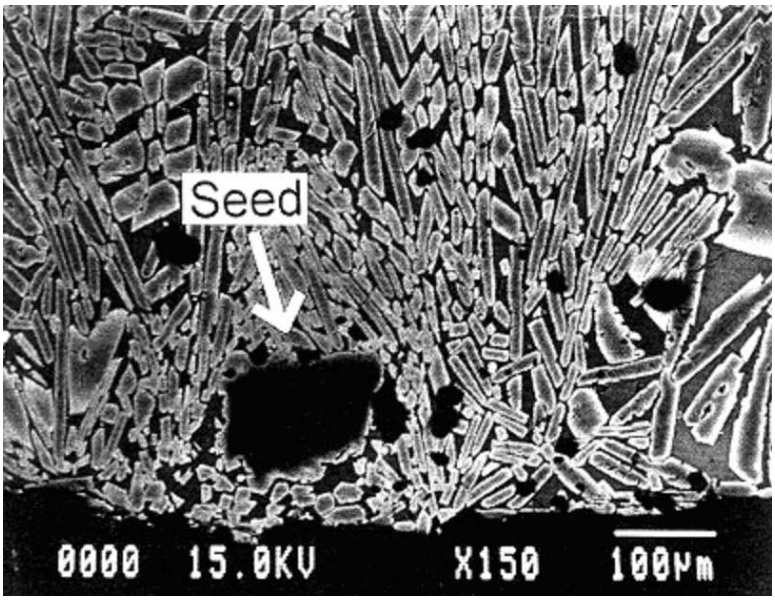

Figure 6. An olivine xenocryst, which has collided with a supercooled melt droplet and induced crystallization of skeletal olivine, resembles but is not strictly a relict grain (Connolly et al. 1998). Type IIA charge heated for 30 min at 1564ºC (liquidus 1546ºC) in IW-0.5, cooled at 500ºC/hr, dust puffed at 1400ºC.

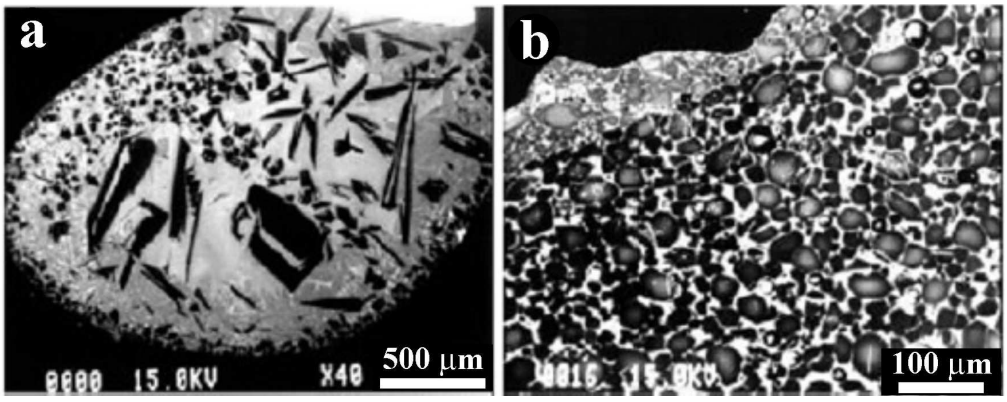

Figure 7. (a) A composite porphyritic olivine spherule, resembling some CR chondrules, which has agglomerated from a mist of microdroplets and grains injected into a furnace during cooling (Yu et al. 1998). (b) A composite spherule aggregated during discontinuous puffing, with an igneous rim resembling those on chondrules for which two heating events have been proposed (Yu & Hewins 1998). See text for experimental details.

Igneous rims on chondrules have been simulated experimentally in a number of ways. Connolly & Hewins (1991) produced accretionary rims by sintering dust to charges at about 1000°C. Partially melted accretionary rims, possibly analogous to igneous rims on chondrules, were produced at higher temperatures (Connolly et al. 1996). Such partially melted rims were made by injecting dust into the furnace so it collided with hot charges, as well as by heating dust-coated spherules (Connolly & Hewins 1991). Note that the occurrence of rims suggests two events because of evidence of reheating of the material underlying the rims in some cases (Krot & Wasson 1995), but rims have also been made in the laboratory in the course of a single heating-cooling event (Connolly & Hewins 1995; Yu et al. 1998).

2.2. Cooling Rates

Cooling rates have been estimated from textures and mineral zoning, and in addition attempts have been made to infer them from concentrations of moderately volatile elements and from the widths of overgrowths on crystals. In many cases, linear cooling rates are discussed, whereas in nature the radiant flux is expected to decline as the fourth power of temperature (Stefan-Boltzmann law). Cooling curves have been used in simulations, particularly motivated initially by the desire to reduce volatile loss at the highest temperatures (Yu & Hewins 1998). Because olivine crystallization takes place over only a few hundred degrees, the textures and mineral zoning are not very sensitive to whether a linear or curved cooling path is used.

A great variety of chondrule textures has been made using cooling rates of 500°C/hr by Connolly et al. (1998), whereas both lower and greater rates have been cited in the older literature for specific types of texture. A recent paper with a comprehensive list of the cooling rates used in experiments which attempted to simulate different kinds of chondrules is by Desch & Connolly (2002), and they can be summarized as 5-3000°C/hr, a range probably larger than the range for the cooling rates of most chondrules. Very different textures can be produced with the same cooling rate because nuclei may or may not be available when cooling begins, depending on combinations of heating time and peak temperature for a given composition (Lofgren 1996). Mineral zoning is a better guide to cooling rate than texture. The upper and lower extremes of cooling rates used in experiments may not necessarily produce good matches to both the textures and the mineral zoning of natural chondrules.

Excentroradial pyroxene textures have been produced with cooling rates up to 3000°C/hr (Hewins et al. 1981), with peak temperatures near the liquidus. However, a peak temperature higher than the liquidus is likely for such compositions with low melting temperatures (Hewins & Radomsky 1990) and, with the more extensive melting at high peak temperatures, nuclei are reduced to embryos so that nucleation will be delayed. Dendritic crystals require rapid cooling when peak temperature is relatively low, but rapid cooling from a high peak temperature is likely to produce glass; thus fine dendrites could be produced for a lower cooling rate with a high peak temperature, and the 3000°C/hr is an upper limit which may not apply to real (superheated) chondrules. Similar arguments apply to BO chondrules, and indeed Tsuchiyama et al. (2004) obtained the best resemblance to natural BO textures with the highest peak temperatures. They favor 1000°C/hr for producing BO textures (Fig. 3), though only limited experiments were made at lower cooling rates.

A potentially more precise way than texture simulation for estimating cooling rate is matching the olivine zoning profiles of chondrules with those for crystals grown in porphyritic charges. Radomsky & Hewins (1990) found a match for cooling rates of 100-1000°C/hr, with no zoning at lower rates. Weinbruch et al. (1998) showed that Fe loss to the Pt support wire suppressed potential zoning in olivine in the 10°C/hr runs of Radomsky & Hewins (1990). Weinbruch et al. (1998) showed olivine zoning for cooling rates of 1-3600°C/hr in their runs with Fe crucibles, but some gain of Fe from the crucible is evident for 10°C/hr and it is strong for 1°C/hr. Jones (1990) pointed out the similar zoning of Semarkona type II chondrule olivine with olivine grown at 100°C/hr. Jones & Lofgren (1993) showed olivine zonation profiles for several cooling rates down to 2°C/hr. The shape of the natural olivine profile, in particular the rapid composition change over the last 20 μm because re-equilibration is less effective at lower temperatures, appears to be closest to the 100°C/hr runs (Fig. 8). Minor element data are also consistent with this cooling rate (Fig. 9). A conservative approach to the simulation of textures and zoning would therefore assign a range of 10-1000°C/hr for cooling rates during chondrule crystallization, with the highest cooling rates for the most supercooled chondrules.

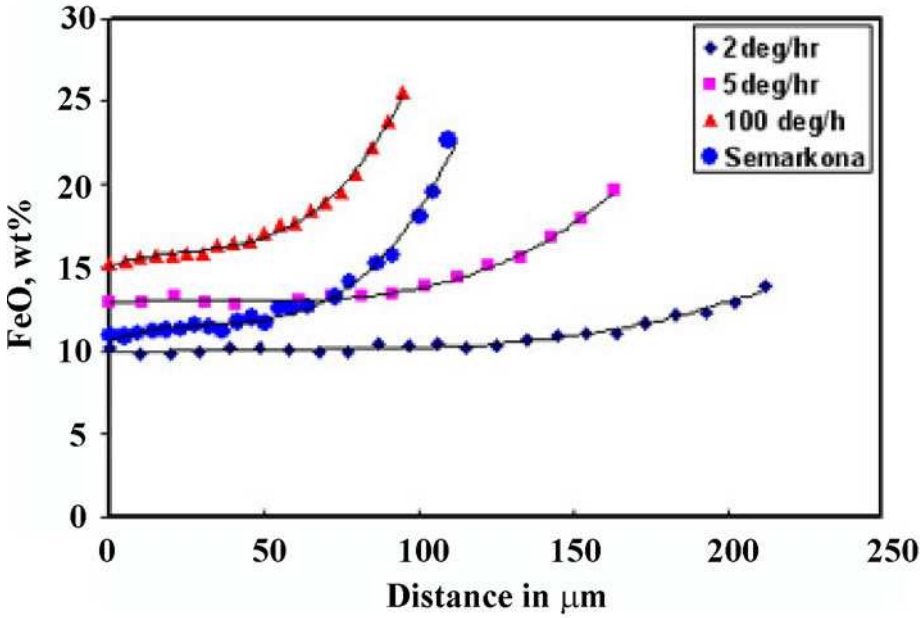

Figure 8. Zoning profiles for olivine grains in three porphyritic olivine charges of type IIA composition and one chondrule (after Jones & Lofgren 1993). Charges were heated for 2 hr 30ºC below or 3 hr 55ºC below the liquidus at IW-0.5.

Attempts have been made to use the partitioning of trace elements (Kennedy et al. 1993; Alexander et al. 1998) and of minor elements (Libourel 1999; Pack &

Palme 2003) between olivine and silicate melt to define chondrule cooling rates. The results showed either no dependence of partition coefficient on cooling rate or a questionable effect possibly due to glass inclusions in the olivine. For instance, the partitioning of Ca and Al between olivine and melt were found to be independent of the cooling rate within the range of 1.5 to 1000°C/h, a plausible range for chondrule formation. Though partition data do not improve our knowledge of cooling rates, Pack & Palme (2003) made the important observation that Ca-rich refractory forsterites found as isolated grains and in some chondrules were not in equilibrium with type IA chondrule melts. They were formed by the crystallization of refractory melts, which were possibly condensates (Pack et al. 2004, 2005). The forsterites could be relicts of refractory chondrules that experienced considerable subsequent condensation diluting the Ca content of the melt (Libourel et al. 2005). Alternatively, the parent refractory melts may well have been the spinel-forsterite-fassaite chondrules described by Zanda et al. (2000, 2005).

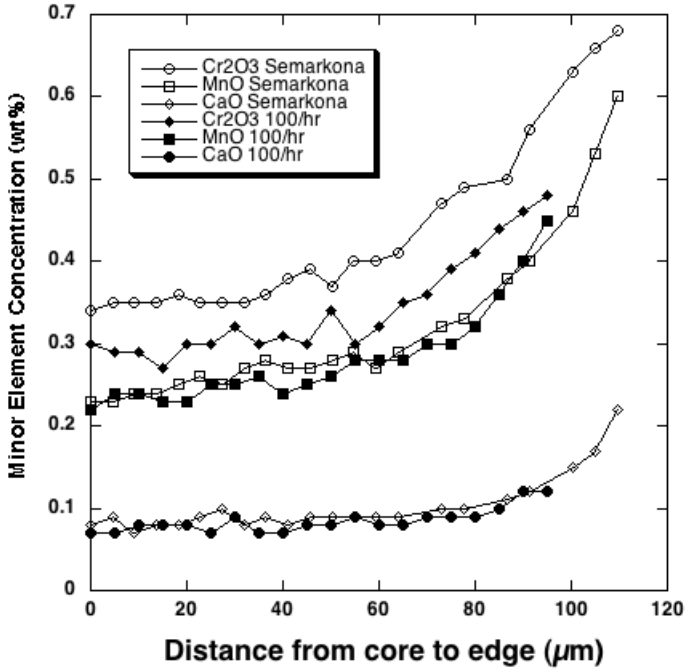

Figure 9. Minor element zoning profiles for olivine in a IIA charge cooled at 100 °/hr and in a chondrule (after Jones & Lofgren 1993; Connolly et al. 2005).

Weinbruch et al. (2001) compared exsolution features in pyroxene for experimental runs on a type IIB chondrule composition (Hewins et al. 1981), as well as

charges of other compositions, with exsolution lamellae in pyroxene from a wide variety of chondrules. In the synthetic samples, coherent exsolution lamellae on {001} were found for cooling rates up to 50-60°C/hr. For higher rates, pyroxenes in charges contained only modulated structures without phase separation. The natural chondrule pyroxenes studied have lamellae, with a range of exsolution wavelengths of 15-85 nm. Compared to lamellae in charges this indicates a cooling rate range of 0.1-50°C/hr. As this applies to temperatures of roughly 1200-1000°C, this is broadly compatible (assuming declining cooling rates according to the Stefan-Boltzmann law) with a range of 10-1000°C/hr for olivine growth, which occurs mostly at higher temperatures.

Wasson & Rubin (2003) and Wasson (2004) proposed that the very thin overgrowths on some relict grains in chondrules must have cooled more quickly than normally zoned phenocrysts. Wasson (2004) argued that the 4-5 μm thickness of the rims on relict grains in the chondrules are about 30× smaller than the grains grown experimentally and the inferred cooling rates should therefore be 1000× larger or about 10^6 °C/hr. Wasson & Rubin (2003) also argued that very small crystals in chondrules were consistent with ultrarapid cooling. There are many experiments in which such textures and overgrowths of the type described by Wasson (2004) have been formed. Lofgren & Le (2000) partially melted crushed ordinary chondrite, and by cooling at a rate of 1000°C/hr produced rather heterogeneous charges containing large magnesian relict grains and small ferroan phenocrysts (Fig. 10), similar to the texture illustrated by Wasson & Rubin (2003). The small grains and the ferroan rims on relicts grew less than 10 μm thick, while cooling at 1000°C/hr. Hewins & Fox (2004) made overgrowths on relict grains during cooling at about 800°C/hr, with thicknesses ranging from sub-micron on the finest starting materials to tens of microns on the coarsest. For powders with <20 μm San Carlos olivine, overgrowths were about 2-6 μm thick for 1470°C (e.g., Fig. 11a) and much thicker for 1550°C, when their abundance was considerably reduced (Fig. 11b). The thickness of olivine rims cannot be used as a cooling rate indicator, as it depends on too many factors (Fox & Hewins 2005). These include surface area of the substrate, i.e. number density or size of crystals, the degree to which the relicts dissolve, the melt composition, and ability of subsequent phases to nucleate, as well as cooling rate.

The high contents of moderately volatile elements, such as alkalis, especially in type II chondrules, have led to an exploration of conditions leading to their loss or retention. Use of non-linear cooling rates initially in the 2000-5000°C/hr range, passing through a series of steps to 250-500°C to avoid growth of too skeletal crystals, allowed the retention of Na at levels similar to those of type II chondrules (Yu & Hewins 1998). However, these experiments were run at a total pressure of 1 atm and a very high oxygen fugacity (f_{O2}). At 10^{-5} atm, a pressure assumed for the solar nebula, Na and K are totally lost by free evaporation in 20-40 minutes at 1450-1485°C (Yu et al. 2003). K isotopic fractionation is observed in these charges but not in natural chondrules. If type I chondrules formed at total pressures predicted to have existed within the protoplanetary disk, and lost K by evaporation, mass fractionation must have been suppressed by exchange between the melt and an ambient gas rich in K, due to evaporation of local dust and molten chondrules (Yu et al. 2003). Na or K loss rates for chondrules scaled for partial pressures in the ambient medium could be used to constrain cooling rates (Beckett & Stolper 1999). Since we do not know the

pressure and composition of the gas in which chondrules formed, we cannot determine their cooling rate from concentrations of volatiles.

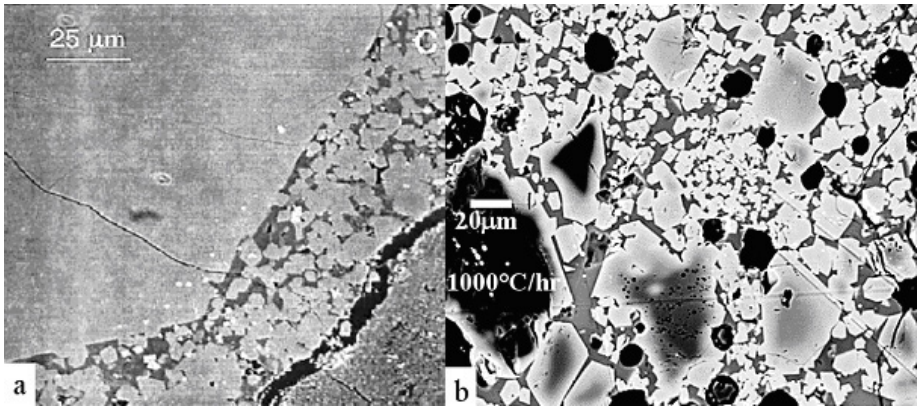

Figure 10. (a) Large and small olivine grains in a chondrule (Wasson & Rubin 2003) and (b) a charge melted for 5 min at 1300°C before cooling at 1000°C/hr (Lofgren & Le 2000).

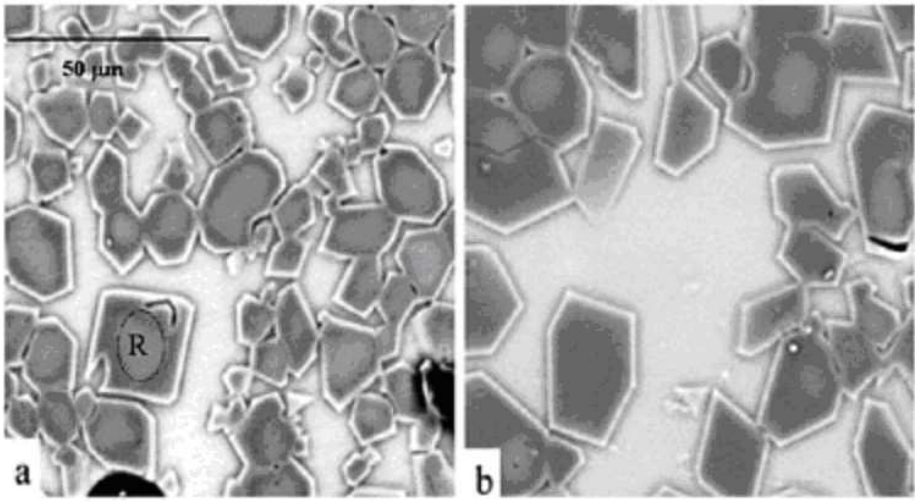

Figure 11. Overgrowths on relict grains (R) about 2-6 μm thick when cooled from 1470°C (a) and much thicker when cooled from 1550°C (b, same magnification), in both cases at about 800°C/hr (Hewins & Fox 2004).

2.3. Peak Temperatures and Heating Times

Heating time and peak temperature both control the number of nuclei surviving from precursor material, meaning that neither can be uniquely defined from textures. The

effect of very rapid heating and cooling on chondrule textures has been studied primarily as a means of conserving alkalis in chondrules. Samples heated by a plasma gun with 10 ms pulses (Hewins et al. 2002) had bubble-rich glass over essentially unaltered unsintered starting material (Fig. 12). The association glass + crystal fragments is reminiscent of the agglutinates formed by micro-impacts on the lunar surface (Basu & Meinschein 1975), but not of chondrules. However, when charges are inserted into a furnace at superliquidus temperature, which is immediately cooled as fast as possible to reach the liquidus, i.e. 1-10 min depending on initial furnace temperature, and subsequently cooled at 500°/hr (Connolly et al. 1998), or heated for one minute at subliquidus temperatures and cooled at about 800°C/hr (Hewins & Fox 2004), textures more appropriate to chondrules are produced. Much closer matches to chondrule textures were produced in crystallization experiments with a time above the liquidus of at least a minute, for any grain size of starting material, than with heating for less than a second.

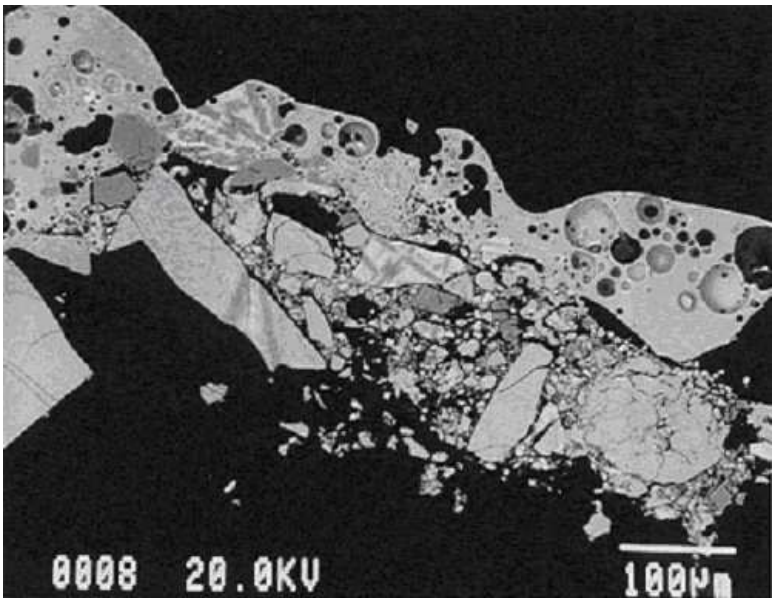

Figure 12. Very short duration heating produces a layer of glass (top) over starting material (bottom) insufficiently heated to be well sintered (Hewins et al. 2000).

Because longer times and higher temperatures have similar effects on eventual textures, we need to pursue other approaches to constrain heating times. Rambaldi (1981) and Jones (1996a) have described reverse zonation in relict olivines in chondrules as a result of diffusion during the partial melting process. This is due to the slow processes of dissolution below the temperatures at which rapid transformation of the olivine to a liquid of the same composition, i.e. congruent melting, would take place (Greenwood & Hess 1996). Experimental diffusion data (e.g., Chakraborty 1997) allow quantitative modeling of the composition profiles across the grains, and this could constrain the heating time precisely, given an estimate of the peak tem-

perature. The reverse zoning in olivine relicts is incompatible with "flash heating" in the most literal sense, which as noted above generates agglutinate-like objects (Hewins et al. 2000), unless the zonation was produced before the grains were incorporated into the chondrules.

The peak heating temperature was estimated by Hewins & Radomsky (1990) as 1400-1750°C, considering the composition limits giving rise to chondrules always totally melted and never totally melted, respectively. Connolly et al. (1998) found that the peak temperature for the transition between porphyritic and barred olivine textures was raised about 100°C for heating times of 1-2 minutes, and the peak temperature range of the barred olivine field broadened. The transition between glass and barred olivine could be pushed up between 100°C and 400°C, for short times above the liquidus, depending on the grain size of the starting material. In view of possible short heating times, the peak temperature range was revised upwards, rather conservatively, to 1500-1850°C by Hewins & Connolly (1996), and a later review of the available data by Jones et al. (2000) led to similar conclusions. For some barred olivines generated from coarse-grained precursors, with specific thermal conditions an upper limit of 2100°C may be possible. Such high temperatures are not likely to be general: BO chondrules become rare at the bulk composition (beyond which all textures are porphyritic) used to define the upper temperature limit; the experiments of Connolly et al. (1996) were done at 1 atm, not at low pressure, and Nagahara & Ozawa (1996) produced BO textures by isothermal evaporation *below* the final liquidus temperature; and Tsuchiyama et al. (2004) found the best approaches to BO texture with peak temperatures 100°C above the (original) liquidus. We therefore adopt a conservative working hypothesis of 1850°C as an upper limit. If the most magnesian porphyritic chondrules achieved their textures as the result of seeding, this would also lead to an underestimation of the maximum temperature.

All the discussion above was based on experiments which behaved to a first approximation as closed systems. Since then it has been experimentally demonstrated that condensation and evaporation may have played a role in forming textures (see below). While temperatures might need to be raised above the original temperature range of Hewins & Radomsky (1990) if the heating time is only of the order of a minute, other considerations also modify this range. If evaporation is important and type IA chondrules were generated by evaporation of a more ferroan spherule heated to subliquidus temperatures to achieve the appropriate number density of crystals, the maximum temperature they reached could have been overestimated by 100-200°C (Cohen et al. 2000, 2004). The most magnesian BO chondrules, however, if formed by evaporation of a less refractory melt, could have been heated to below their final liquidus temperature of 1750°C (Nagahara & Ozawa 1996). BO textures more similar to those of natural chondrules are produced for superliquidus temperatures (Tsuchiyama et al. 2004). Finally, there are rare objects interpreted as slightly melted chondrules, including dark-zoned chondrules and protoporphyritic chondrules, with peak temperatures as low as 1300°C (Lofgren & Le 2000).

3. Chemical Exchange Experiments

The array of chondrule bulk compositions might be explained by virtually closed-system melting of precursors of different composition primarily due to prior nebular

processes (e.g., Grossman 1988). However, there is an alternative approach to chondrule formation, involving exchange during melting with the low-pressure gas of the nebula. The array of chondrule bulk compositions may have been acquired by evaporative losses to (Sears et al. 1996; Cohen et al. 2004), or gains from (condensation or dust accretion) the surrounding medium (gas or/and dust) during the chondrule forming-event (e.g., Libourel et al. 2005). While growing evidence argues for such exchanges (Zanda 2004), we also note that no consensus exists on the extent to which chondrules reacted with the surrounding medium, nor on the effects of such interactions on chondrule characteristics. In order to address this question, several experimental efforts have been undertaken to better understand elemental and isotopic fractionations in chondrules due to evaporation (e.g., Floss et al. 1996) and due to condensation and gas-solid or gas-melt reactions (e.g., Tissandier et al. 2002).

The evaporative loss of elements, such as sodium and sulfur, at high temperature is well known, even in experiments conducted at 1 bar total pressure, and in relatively oxidizing atmospheres. Therefore presence of such elements in chondrules, which probably formed at total pressures much lower than 1 bar in the solar nebula, presents us with an opportunity to clarify their formation conditions through experiments performed at total pressures lower than 1 bar. This is complicated by the fact that re-entry of volatile elements happened at both low and high temperatures (Yu et al. 2003; Grossman & Alexander 2004). The survival of chondrules is significant, as silicate melts are not stable at all when a gas of solar composition at 10^{-3} to 10^{-5} bars is cooled, as is clear from both theoretical and experimental data (e.g., Wood & Hashimoto 1993; Wang et al. 2003). On the other hand, if the gas is highly enriched in the lithophile elements relative to hydrogen, e.g., as a result of heating and evaporation of a dust concentration, melts fairly similar to chondrules in composition can condense (Ebel & Grossman 2000). This has led to the development of new experimental systems for studying condensation related to chondrule formation. We also treat here experiments related to the gain or loss of oxygen by chondrules, involving reduction of chondrule silicates and isotopic exchange with ambient gas.

3.1. Evaporation Experiments

In the quest to comprehend chondrule formation processes, significant experimental efforts have been expended to unravel the behavior of moderately volatile elements in chondrules, and notably the factors that control their concentrations in chondrule melts. Amongst these elements, alkalis have received much attention because they are volatile lithophiles, and hence may help us to put some valuable constraints on chondrule formation processes. Tsuchiyama et al. (1981) demonstrated that Na loss increases as a function of isothermal heating time, increasing temperature, and decreasing oxygen fugacity at 1 atm pressure. Yu & Hewins (1998) conducted similar experiments but, instead of being heated isothermally, charges were given one minute to reach furnace temperature and then were cooled along various steep T/t curves. They found greater losses for higher peak temperatures, lower cooling rates, and lower f_{O2}. There is also a bulk composition effect, with greater Na loss for higher Mg content of the melt, the activity of Na being affected by melt polymerization. Na loss was found to be lower for higher ambient P_{Na}, by comparing experiments where the furnace gas was flowing to those where it was static. Yu & Hewins (1998) showed

that the high Na contents of type II chondrules could be explained by brief heating and rapid cooling, but only if the f_{O2} was very high (corresponding to 1000× dust enrichment in the gas before evaporation) and the total pressure was at least 1 atm.

Subsequently, Yu et al. (2003) reinvestigated isothermal loss of alkalis from chondrule composition melts in a vacuum furnace. With nebular pressures, effectively all Na and K are lost in about 40 minutes in residual air (Fig. 13) or 20 minutes in H_2, though Na is lost faster than K, whereas FeO is lost much more slowly (Cohen et al. 2004). Based on these results, any chondrule that experienced evaporation of FeO within a canonical nebula should be Na-free. Silicate melts heated at 10^{-5} bars in residual air show the predicted Rayleigh fractionation of K isotopes. However, K isotopic fractionation showed a negative correlation with pressure, and is minimal at 1 atm, because of exchange with the ambient gas. Cohen et al. (2004) showed that the extent of isotopic fractionation of K from a silicate melt at a P_{H2} of 1.3×10^{-7} bars could be reduced by allowing the K gas to accumulate in a covered crucible (Fig. 14).

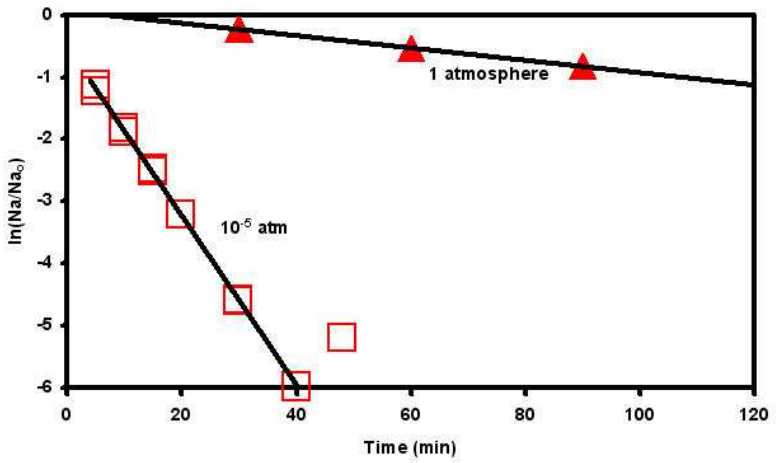

Figure 13. Fraction of Na retained in K-enriched type IIAB analog chondrule melts at 1450ºC, as a function of pressure (of CO-CO_2 IW-0.5 at 1 atm, or residual air at 10^{-5} atm) and time (Yu et al. 2003).

Yu et al. (1996) investigated S loss from chondrule-like melts at 1 atm total pressure and no ambient S species in the vapor. S loss is not complete if the charges are heated to 1500°C or less for one minute and then cooled rapidly. Silicate charges containing troilite heated at 1350°C and P_{H2} of 1.3×10^{-5} bars, took between 2 minutes and 10 minutes to lose all their sulfur (Cohen & Hewins 2004). Application of such data to natural chondrules is difficult, because the total pressure of the ambient gas and the partial pressures of the S species are not known.

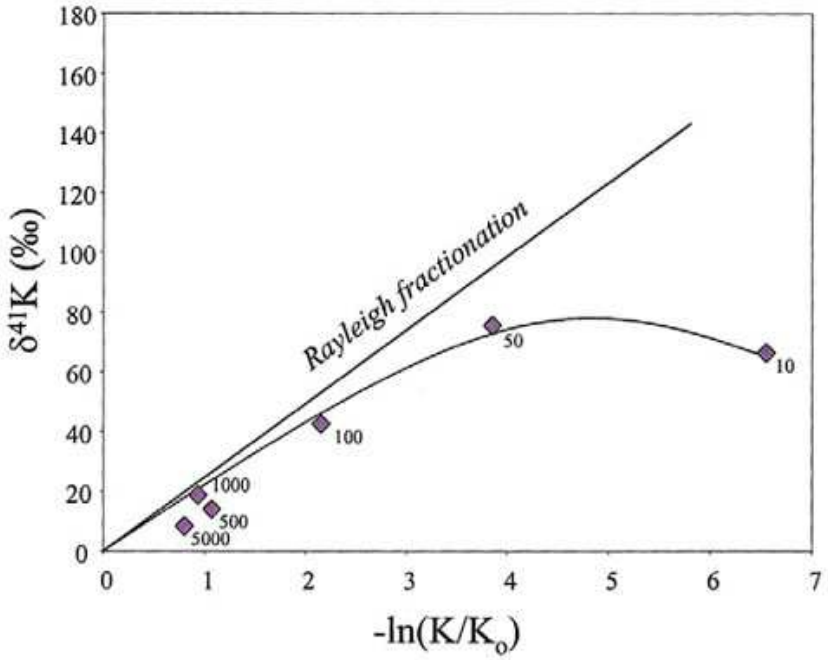

Figure 14. Fraction of K retained and isotopic composition for charges heated at a P_{H2} of 1.3×10^{-7} bars in covered capsules, as a function of cooling rate between 5000°C/hr and 10°C/hr. K isotopic fractionation is partially suppressed for low cooling rates because of back reaction with the ambient gas (Cohen et al. 2004).

Evaporation experiments were conducted by Cohen et al. (2004) on an anhydrous CI-composition starting material (initial liquidus temperature ~1633ºC) to see whether the chemical compositions of the various chondrule types could be derived (Fig. 15a). Porphyritic olivine spherules were produced at 1580ºC and P_{H2} of 1.3×10^{-5} atm and then quenched. The oxygen fugacity was controlled by the gas escaping from the melt. The olivine attempting to maintain equilibrium with the evaporating melt is initially similar to olivine in type IIA chondrules, but with FeO loss over 12-18 hours it became ~Fo_{99}, similar to that in type IA chondrules. The CaO-MgO and CaO-FeO trends in the olivine match the trends for natural chondrules (Fig. 15b). This correlation shows that evaporation of CI precursors could generate some chondrules but, though it is not apparent from this figure, silica-rich ones (IIB and IB) would require a more pyroxene-rich precursor. Mass fractionation of Si isotopes is observed in the charges, but not in natural chondrules. The absence of mass fractionation, like the presence of alkalis, can be reconciled with evaporation, if the chondrules were embedded in a gas with high partial pressures of the lithophile elements or high total pressure (Georges et al. 2000; Cohen et al. 2004). The loss of iron from silicate melt scaled for chondrule size would take about 3 hr with canonical conditions but longer in a gas with the high P_{Fe} needed to suppress mass fractionation.

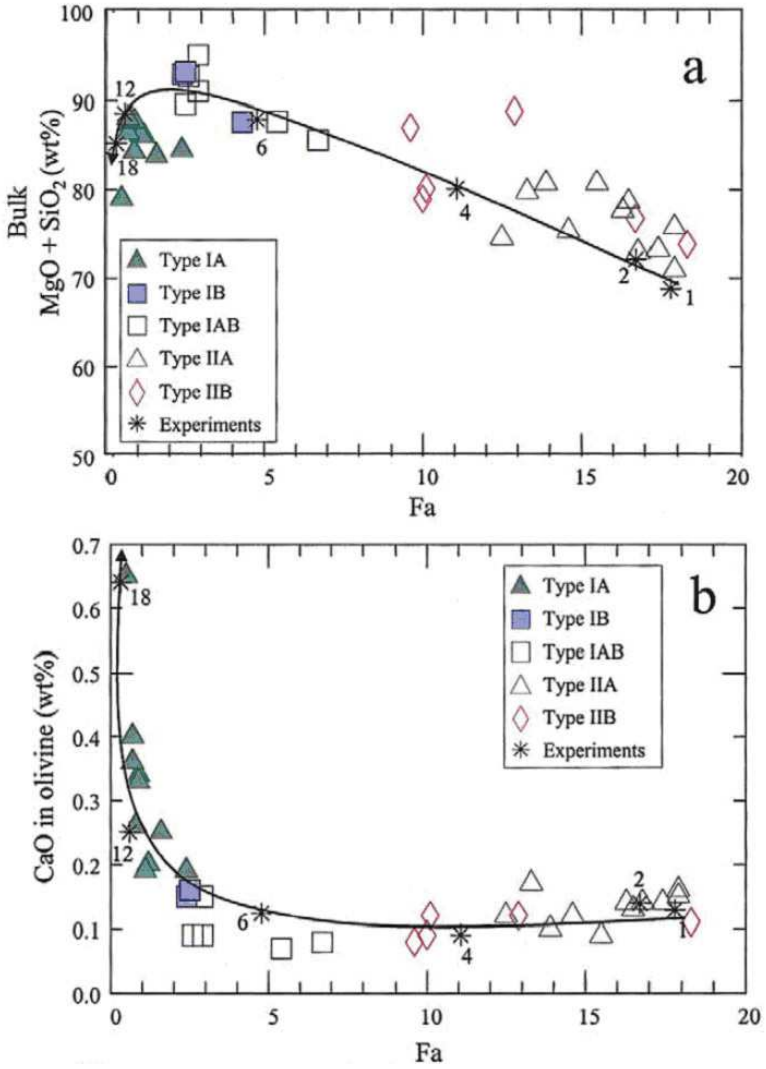

Figure 15. Comparison of ($MgO+SiO_2$) in the bulk (a) and CaO in olivine (b) as a function of Fe content of olivine (Fa), for chondrules (Jones 1996, and references therein) and charges evaporated at 1580ºC for 1 to 18 hr (numbers beside runs) in hydrogen at 1.3×10^{-5} bars (Cohen et al. 2004).

3.2. Condensation Experiments

Most evaporation experiments do not take into account the effect of partial pressure of alkalis in the surrounding nebular gas, which, in turn, may drastically affect the rate of volatilization and condensation of alkalis in molten chondrules. Therefore, to

quantify how an alkali-rich vapor might affect alkali behavior in chondrules, new experiments were designed to expose silicate melt samples to a controlled alkali partial pressure at high temperature under a fixed oxygen fugacity. Lewis et al. (1993) heated molten basalt in a high partial pressure of Na, achieved by evaporating NaCl in the furnace. Under conditions where otherwise over 80% of the Na would be lost from the basalt, many runs actually gained Na with exposure to this gas for 16 hours at 1330°C, due to condensation. Georges et al. (2000) performed similar 1 atm experiments on K condensation into a CMAS liquid, deriving the K by reduction of K_2CO_3 by graphite. The equilibrium concentrations of K for partial pressures of K close to 10^{-3} atm were achieved in 1-2 hours at 1410°C (Fig. 16a), while a K-rich melt evaporated to reach the same composition in the same time. The K isotopic composition of the charge also reaches an equilibrium value when saturation in K is achieved during condensation (Fig. 16b). This was taken to be the composition of the gas when saturation occurs, and subsequent isotopic exchange between the gas, whose isotopic composition should continue to evolve, and the melt appears to be inefficient (Georges et al. 2000). From these two results, we see that alkalis entering chondrules from the nebular gas is a viable mechanism to explain the chondrule alkali contents and their $\delta^{41}K$ isotopic signatures, at time scales relevant to chondrule formation, though alkalis also entered chondrules at low temperatures. Given the lower pressures of alkalis in the nebula, we would expect heating times of chondrules to be longer than in these experiments.

The approach of Georges et al. (2000) was adapted to low pressure condensation by Tissandier et al. (2002), who used a source of quartz and graphite to generate SiO vapor. SiO impinged on and entered CMAS charges producing a gradient in the SiO_2 content from center to edge of 55 to 60% in the case of a totally molten charge. Charges containing olivine and melt changed their characteristics as a result of condensation of silica. Condensation for 2 to 5 minutes at 1350-1450°C and 10^{-1} atm CO produced a chemical and mineralogical zonation in the charges. Olivine was replaced by pyroxene as the major phase towards the margin of the charges, and in some cases the rim contained a silica polymorph (Fig. 17). Charges which grew pyroxene around the rim as the result of the influx of Si resemble type IAB chondrules (Scott & Taylor 1983). By contrast, charges cooled without SiO in the ambient gas did not nucleate pyroxene until the temperature was lowered, and then throughout the charge, not just at the margin. The multiple zonation in silica-rich phases found in some charges resembles what is seen in some layered chondrules, particularly in CR chondrites (Fig. 18; and Krot et al. 2004). Direct condensation of $SiO_{(gas)}$ into chondrule melt, and the observed increase of pyroxene/olivine ratios towards the peripheries of most Type I chondrules in CR, CV and ordinary chondrites, may explain the origin of pyroxene-rich chondrules in general.

3.3. Oxygen Isotopes

Chondrules show signs of exchange of oxygen isotopes with an isotopically heavier gas. They contain fairly heterogeneous olivine, including relict grains with oxygen lighter than that of melt-grown crystals (Yurimoto & Wasson 2002; Jones et al. 2004). The ^{16}O-rich grains are possibly related to refractory inclusion olivine or condensate olivine, which were exchanging with the melt. The experimental study of

these exchange reactions could shed light on chondrule formation conditions. Yu et al. (1995) found that a silicate melt could exchange 50% of its oxygen in 5 minutes with ambient water vapor, but this was at 1 atm total pressure. They concluded that extended heating would be required in the nebula, or many heating events. Exchange experiments by Boesenberg et al. (2004) show that elimination of an isotopic signature in a large relict grain by reaction with melt, without the influence of the high pressure gas, would take an hour or more at 1500°C. This approach may eventually lead to constraints on chondrule thermal history.

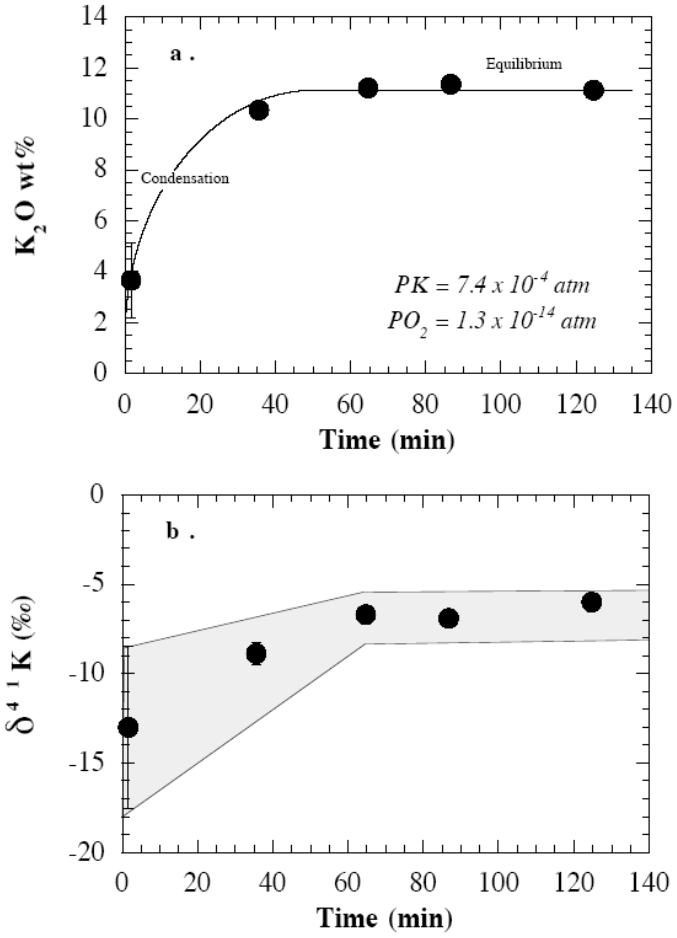

Figure 16. Mean K contents and K isotopic composition as a function of time for silicate melts heated in a K-rich atmosphere (Georges et al. 2000). The shaded lines indicate maximum and minimum values of measurements.

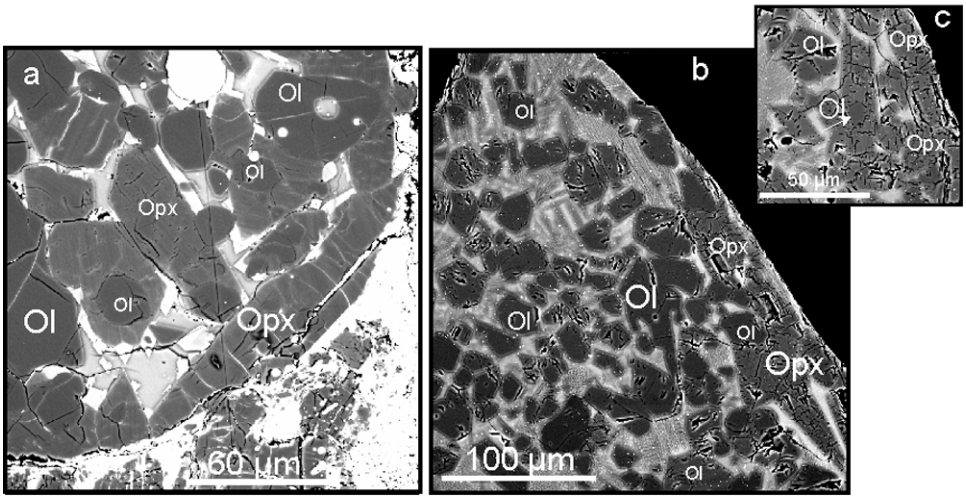

Figure 17. a) Low-Ca pyroxene formed on the edge of a Semarkona POP Type I chondrule and b) a charge held for a few minutes at 1400°C in an SiO-CO-rich atmosphere (Tissandier et al. 2002). c) Detail of the same experimental charge showing olivine poikilitically enclosed into low-Ca pyroxene.

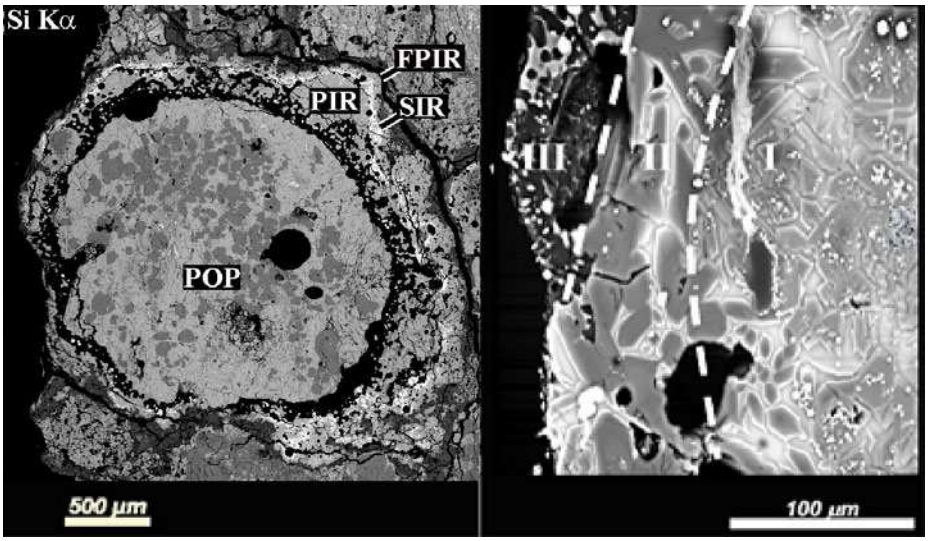

Figure 18. Concentric zonation in a POP chondrule (left, Si x-ray image) surrounded by Fe metal (black), pyroxene-rich igneous rims (PPIR, PIR), and a Si-rich igneous rim (SIR, white). A charge held at 1400ºC for a few minutes in an SiO-rich atmosphere (right, BSE) shows a similar sequence of I olivine, II low-Ca pyroxene and III a silica polymorph (black) corresponding to a gradient in silica (Tissandier et al. 2002).

3.4. Fe Reduction

Since formation of metal in chondrules may involve loss of S or O to the ambient gas, we treat this topic here. Of particular interest are olivine grains with Fe inclusions, apparently formed by the reduction of ferroan olivine recycled from chondrules (Jones & Danielson 1997). Reduction of olivine or chondrule proxies at 1350-1610ºC by C usually as graphite (Connolly et al. 1994; Libourel & Chaussidon 1995; Lemelle et al. 2001; Leroux et al. 2003) produced assemblages of dusty olivine (Fo-rich olivines with small metal inclusions) and Fe-Ni metal globules in silicate glass, with textural features very similar to those observed in chondrules. Large metallic blebs (1 to 50 μm), located in the silicate melt at the olivine grain boundaries, and tiny Fe metal inclusions (<1μm) in olivine, at 1 atm (Connolly et al. 1994; Lemelle et al. 2001; Lofgren & Le 2002a,b; Leroux et al. 2003) and at 1.3×10^{-5} atm H_2 pressure (Cohen & Hewins 2004) mimic both the metal in the mesostasis and the dusty olivine relict grains found in many chondrules. Micron-sized metal blebs observed in dusty regions often show preferential alignments along crystallographic directions of the olivine grains, have low Ni contents (typically < 2 wt%), and are frequently surrounded by a silica-rich glass layer (Leroux et al. 2003). The reduction products are fairly similar whether single olivine crystals are partially melted or whether the olivine is within a chondrule melt analogue. Ignoring the reducing agent, the breakdown of the olivine can be expressed as:

$$Fe_2SiO_{4\ \text{in olivine}} = 2Fe_{\ \text{metal}} + x\ SiO_{2\ \text{in melt}} + (1\text{-}x)\ SiO_{\ \text{in gas}} + (3\text{-}x)/2\ O_{2\ \text{in gas}}$$

Some volatilization of SiO gas may account for the departure of the Fe and Si in metal and glass from olivine stoichiometry, observed in both experimental and natural samples (Leroux et al. 2003). Comparison with experiments suggests that time scales of the order of minutes are adequate for metal formation. The reduction and volatilization probably occur at peak temperatures, and may be followed by recondensation of Si during cooling.

Reduction of FeO to metal as discussed above is more rapid than loss of Fe from silicate melt by evaporation. Evaporation of Fe from metal occurs at a significant rate even at 1 bar: metal was no longer present after 12 hours heating of 4mm chondrule analogs at 1580°C at 1 atm IW-3, because of evaporation (Cohen & Hewins 2004). At the same temperature with a P_{H2} of 10^{-5} bar (<IW-4.8 but charge self-buffered), loss of Fe from the silicate melt by evaporation takes 18 hours for 4mm charges and no Fe metal is formed (Cohen et al. 2004; Cohen & Hewins 2004). At temperatures that produce extensive melting within chondrules at total pressures of less than 1 bar, the stable form of Fe is vapor (Wood & Hashimoto 1993). The vapor pressure of Fe at the temperatures of interest is $\sim10^{-4}$ bars (Cohen & Hewins 2004). The presence of Fe metal in chondrules requires some combination of high total pressure P_T, high P_{Fe} and short heating time, unless the metal is armored inside olivine crystals.

Several other aspects of metal behavior in experiments are relevant to chondrule compositions. Work by Connolly et al. (2002) has determined that some metal within the matrix of CR2 chondrites was produced within chondrules and expelled. Metal and silicate melt droplets separate from each other with ease in static furnace experiments (e.g., McCoy et al. 1999), which may be relevant to the metal droplets found in chondrites. The effect of motion within the chondrule and perhaps rejection of phases

(e.g., spinning droplets) could potentially be attacked through levitation experiments. There is also a kinetic isotope effect in the reduction of silicate melt to Fe metal (Cohen et al. 2005), which may be relevant to Fe isotopic variation in chondrules.

4. Summary

Chondrule-like spherules have been formed in the lab in several distinct processes: partial to complete melting of mineral aggregates, with or without a role for partial evaporation or partial condensation, inserting mineral grains into totally molten spheres, and accumulating melt microdroplets and crystals into globules. Condensation of synthetic chondrules from gas is in principle possible but has not yet been achieved.

Very specific formation conditions cannot be given for chondrules, without knowledge of exactly what the heating mechanism was. When a standard model emerges, we should be able to define temperatures and times for it. For closed-system heating for long times (many minutes to a few hours), the peak temperature range would have been about 1400-1750°C. For very short heating times (less than a few minutes), the range would have been higher, about 1500-1850°C. If extensive evaporation was important, the upper limit for porphyritic olivine chondrules would be much lower, because the final liquidus temperature would be much higher than the original one, and the range about 1400-1600°C. The heating time could be from about a minute to many hours. Cooling rates were probably in the range 10-1000°C/hr for the crystallization interval, based on olivine zoning. The thickness of overgrowths on crystals cannot be used to obtain reliable cooling rates.

A chondrule melt in a hot gas at ~10^{-5} bars experiences exchange between the two phases, depending on the composition of the gas. It is likely that evaporation accompanied melting, and recondensation accompanied crystallization, though it is difficult to generalize about the relative extents. If chondrules experienced evaporation, high partial pressures of lithophile elements would have been necessary to suppress mass fractionation. If chondrules experienced condensation during formation, again high partial pressures would have been required. Pressures of S and K have been estimated in the range 10^{-3} to 10^{-6} bars (Beckett & Stolper 1996; Georges et al. 2000). For either evaporation or condensation, formation times would be long because equilibration, particularly isotopic exchange for K and O, evaporation of FeO and diffusion in of alkalis, requires heating for hours. The strong enrichments of lithophile elements in the gas over canonical values requires that solids be concentrated relative to gas before heating. This in turn implies that chondrule formation was on a very local scale, such as in a dusty midplane, in clumps or in association with asteroidal bodies.

Interactions between nebular gas and molten silicates could have played a major role in the formation and fractionation of the first solids formed in the solar system (Libourel et al. 2005), and clearly more work needs to be done in this direction. Specifically, experiments with melting, crystallization, evaporation and condensation, in which complex gas partial pressures are controlled, are needed.

Acknowledgments. RHH thanks the CNRS Institut National des Sciences de l'Univers for a position of Chercheur Associé, and the Université Blaise Pascal for a position

of Professeur Invité. He also acknowledges hospitality from François Robert at the Muséum National d'Histoire Naturelle, Paris, where this chapter was written, and from Betrand Devouard at the Labo. Magmas et Volcans, where it was revised. We thank A. Krot and B. Zanda for images. The paper was critically reviewed by J. Beckett, R. H. Jones, and A. Krot.

References

Alexander, C. M. O'D., & Hewins, R. H. 2004, Meteorit. Planet. Sci., 39 Suppl., A13
Alexander, C. M. O'D., Yu, Y., Wang, J., & Hewins, R. H. 1998, Lunar Planet. Sci., 29, 1775
Basu, A., & Meinschein, W. G. 1975, Proc. Lunar Planet. Sci. Conf., 7, 337
Beckett J. R., & Stolper, E. M. 2001, Lunar Planet. Sci., 32, 1730
Boesenberg, J. S., Hewins, R. H., & Chaussidon, M. 2004, http://www.lpi.usra.edu/meetings/chondrites2004/pdf/9047.pdf
Chakraborty, S. 1997, J. Geophys. Res., 102, B6:12317
Cohen, B. A., & Hewins, R. H., 2004, Geochim. Cosmochim. Acta, 68, 1677
Cohen, B. A., Hewins, R. H., & Yu,Y. 2000, Nature, 406, 600
Cohen, B. A., Hewins, R. H., & Alexander, C. M. O'D. 2004, Geochim. Cosmochim. Acta, 68, 1661
Cohen, B. A., Levasseur, S., Zanda, B., Hewins, R. H., & Halliday, A. N. 2005, Lunar Planet. Sci., 36, 1690
Connolly, H. C. Jr., & Desch, S. J. 2004, Chem. Erde, 64, 95
Connolly, H. C. Jr., & Hewins, R. H. 1991, Lunar Planet. Sci., 22, 233
Connolly, H. C. Jr., & Hewins, R. H. 1991, Geochim. Cosmochim. Acta, 55, 2943
Connolly, H. C. Jr., & Hewins, R. H. 1995, Geochim. Cosmochim. Acta, 59, 3231
Connolly, H. C. Jr., & Hewins, R. H. 1996, Lunar Planet. Sci., 27, 247
Connolly, H. C. Jr., & Hewins, R. H. 1996, in Chondrules and the Protoplanetary Disk, eds. R. H. Hewins, R. H. Jones, & E. R. D. Scott (Cambridge: Cambridge Univ. Press), 129
Connolly, H. C. Jr., & Jones, R. H. 2005, Lunar Planet. Sci., 26, 1881
Connolly, H. C. Jr., Huss, G. R., & Wasserburg, G. J. 2001, Geochim. Cosmochim. Acta, 65, 4567
Connolly, H. C. Jr., Hewins, R. H., Ash, R. D., Zanda, B., Lofgren, G. E., & Bourot-Denise, M. 1994, Nature, 371, 136
Connolly, H. C. Jr., Jones, B. D., & Hewins, R. H., 1998, Geochim. Cosmochim. Acta, 62, 2725
Desch, S. J., & Connolly, H. C. Jr. 2002, Meteorit. Planet. Sci., 37, 183
Ebel, D. S., & Grossman, L. 2000, Geochim. Cosmochim. Acta, 64, 339
Fagan, T. J. et al. 2002, Meteorit. Planet. Sci., 37, 371
Faure, F., Trolliard, G., Nicollet, C., & Montel, J.-M. 2003, Contrib. Mineral. Petrol., 145, 251
Floss, C., El Goresy, A., Zinner, E., Kransel, G., Rammensee, W., & Palme, H. 1996, Geochim. Cosmochim. Acta 60, 1975
Fox, G. E., & Hewins, R. H. 2005, Geochim. Cosmochim. Acta 69, 2441
Georges, P., Libourel, G. & Deloule, E. 2000, Meteorit. Planet. Sci. 35, 1183
Greenwood, J. P., & Hess, P. C. 1996, in Chondrules and the Protoplanetary Disk, eds. R. H. Hewins, R. H. Jones, & E. R. D. Scott (Cambridge: Cambridge Univ. Press), 205
Grossman, J. N. 1988, in Meteorites and the Early Solar System, eds. J. F. Kerridge & M. S. Matthews (Tucson: Univ. Arizona Press), 681
Grossman, J. N., & Alexander, C. M. O'D. 2004, Meteorit. Planet. Sci., 39, 5161
Hewins, R. H. 1988, in Meteorites and the Early Solar System, 1988, eds. J. F. Kerridge & M. S. Matthews (Tucson: Univ. Arizona Press), 73

Hewins, R. H. 1997, Ann. Rev. Earth Planet. Sci., 25, 61
Hewins, R. H., & Connolly, H. C. Jr. 1996, in Chondrules and the Protoplanetary Disk, eds. R. H. Hewins, R. H. Jones, & E. R. D. Scott (Cambridge: Cambridge Univ. Press), 197
Hewins, R. H., & Fox, G. E. 2004, Geochim. Cosmochim. Acta, 68, 917
Hewins, R. H., & Radomsky, P. M. 1990, Meteoritics, 25, 309
Hewins, R. H., Klein, L. C., & Fasano B. V. 1981, Proc. Lunar Planet. Sci. Conf., 12, 123
Hewins, R. H., Yu, Y., Zanda, B., & Bourot-Denise, M. 1997, Antarct. Met. Research, 10, 294
Hewins, R. H., Zanda, B., Horanyi, M., Robertson, S., Den Hartog, D. G., & Fiskel, G. 2000, Lunar Planet. Sci., 31, 1675
Jones, R. H. 1990, Geochim. Cosmochim. Acta, 54, 1785
Jones, R. H. 1996a, in Chondrules and the Protoplanetary Disk, eds. R. H. Hewins, R. H. Jones, & E. R. D. Scott (Cambridge: Cambridge Univ. Press), 163
Jones, R. H. 1996b, Geochim. Cosmochim. Acta, 60, 3115
Jones, R. H., & Lofgren, G. E. 1993, Meteoritics, 28, 213
Jones, R. H., Lee, T., Connolly, H. C. Jr., Love, S. G., & Shang, H. 2000, in Protostars and Planets IV, eds. V. Mannings, A. P. Boss, & S. S. Russell (Tucson: University of Arizona Press), 927
Jones, R. H., Leshin, L. A., Guan, Y., Sharp, Z. D., Durakiewicz, T., & Schilk, A. J. 2004, Geochim. Cosmochim. Acta, 68, 3423
Kennedy, A. K., Lofgren, G. E., Wasserburg, G. J. 1993, Earth Planet. Sci. Lett., 115, 177
Krot, A. N., & Wasson, J. T. 1995, Geochim. Cosmochim. Acta, 59, 4951
Krot, A. N., Meibom, A., Russell, S. S., Alexander, C.M. O'D., Jeffries, T. E., & Keil K. 2001, Science, 291, 1776
Krot, A. N., Libourel., G., Goodrich, C. A., & Petaev, M. I., 2004, Meteorit. Planet. Sci., 39, 1931
Lemelle, L., Guyot, F., Leroux, H., & Libourel. G. 2001, Amer. Mineral., 86, 47
Leroux, H., Libourel, G., Lemelle, L., & Guyot, F. 2003, Meteorit. Planet. Sci., 38, 81
Lewis, R. D., Lofgren, G. E., Franzen, H. F., & Windom, K. E. 1993, Meteoritics, 28, 622
Libourel, G. 1999, Contrib. Mineral. Petrol., 136, 63
Libourel, G., & Chaussidon, M. 1995, Meteoritics, 30, 536
Libourel, G., Krot, A. N., & Tissandier, L. 2005, Lunar Planet. Sci., 36, 1877
Lofgren, G. E. 1989, Geochim. Cosmochim. Acta, 53, 461
Lofgren, G. E. 1996, in Chondrules and the Protoplanetary Disk, eds. R. H. Hewins, R. H. Jones, & E. R. D. Scott (Cambridge: Cambridge Univ. Press), 187
Lofgren, G. E., & Russell, W. J. 1986, Geochim. Cosmochim. Acta 50, 1715
Lofgren, G. E., & Le, L. 2000, Lunar Planet. Sci., 31, 1809
Lofgren, G. E., & Le, L. 2002a, Lunar Planet. Sci., 33, 1612
Lofgren, G. E., & Le, L. 2002b, Meteorit. Planet. Sci., 37 Suppl., A90
Lofgren, G. E., Le, L., & Schatz, V. 1999, Lunar Planet. Sci., 30, 1742
McCoy, T. J., Dickinson, T. L., & Lofgren, G. E. 1999, Meteorit. Planet. Sci., 34, 735
McSween, H. Y. Jr. 1977, Geochim. Cosmochim. Acta, 41, 1843
Nagahara, H. 1996, Lunar Planet. Sci., 27, 927
Nelson, L. S., Blander, M., Skaggs, S. R. & Keil, K. 1972, Earth Planet. Sci. Lett., 14, 338
Nettles J., Le, L., Lofgren, G. E., & McSween, H. Y. Jr. 2003, Lunar Planet. Sci., 34, 182
Pack, A., & Palme, H. 2003, Meteorit. Planet. Sci., 38, 1263
Pack, A., Yurimoto, Y., & Palme, H. 2004, Geochim. Cosmochim. Acta, 68, 1135
Pack, A., Palme, H., & Shelley, J. M. G. 2005, Geochim. Cosmochim. Acta, in press
Radomsky, P. M., & Hewins, R. H. 1990, Geochim. Cosmochim. Acta, 54, 3475
Rambaldi, E. R. 1981, Nature, 293, 558
Scott, E. R. D., & Taylor, G. J. 1983, Proc. Lunar Planet. Sci. Conf., 14, B275

Scott, E. R. D., & Krot, A. N. 2005, ApJ, 623, 571
Sears, D. W. G, Huang, S., & Benoit, P. H. 1996, in Chondrules and the Protoplanetary Disk, eds. R. H. Hewins, R. H. Jones, & E. R. D. Scott (Cambridge: Cambridge Univ. Press), 221
Tissandier, L., Libourel, G., & Robert, F. 2002, Meteorit. Planet. Sci., 37, 1377
Toppani, A., & Libourel, G. 2003, Geochim. Cosmochim. Acta, 67, 4621
Tsuchiyama, A., Nagahara, H., & Kushiro, I. 1981, Geochim. Cosmochim. Acta, 45, 1357
Tsuchiyama, A., Osada, Y., Nakano, T., & Uesugi, K. 2004, Geochim. Cosmochim. Acta, 68, 653
Wang, J., Davis, A. M., Clayton, R.N., Mayeda, T. K., & Hashimoto, A. 2001, Geochim. Cosmochim. Acta, 65, 479
Wasson, J. T. 2004, http://www.lpi.usra.edu/meetings/chondrites2004/pdf/9113.pdf
Wasson, J. T., & Rubin, A. E. 2003, Geochim. Cosmochim. Acta, 67, 2239
Weinbruch, S., Buttner, H., Rosenhauer, M., & Hewins, R. H. 1998, Meteorit. Planet. Sci., 33, 65
Weinbruch, Müller W. F., & Hewins, R. H. 2001, Meteorit. Planet. Sci., 36, 1237
Weisberg, M. K., & Prinz, M. 1996, in Chondrules and the Protoplanetary Disk, eds. R. H. Hewins, R. H. Jones, & E. R. D. Scott (Cambridge: Cambridge Univ. Press), 119
Wood, J. A. 1996, in Chondrules and the Protoplanetary Disk, eds. R. H. Hewins, R. H. Jones, & E. R. D. Scott (Cambridge: Cambridge Univ. Press), 55
Wood, J. A., & Hashimoto, A. 1993, Geochim. Cosmochim. Acta, 57, 2377
Yu, Y., & Hewins, R. H. 1998, Geochim. Cosmochim. Acta, 62, 159
Yu, Y., Hewins, R. H., Clayton, R. N., & Mayeda, T. K. 1995, Geochim. Cosmochim. Acta, 59, 2095
Yu, Y., Hewins, R. H., Alexander, C. M. O'D., & Wang, J. 2003, Geochim. Cosmochim. Acta, 67, 773
Yurimoto, H., & Wasson, J. T. 2002, Geochim. Cosmochim. Acta, 66, 4355
Yu, Y., Hewins, R. H., & Zanda, B. 1996, in Chondrules and the Protoplanetary Disk, eds. R. H. Hewins, R. H. Jones, & E. R. D. Scott (Cambridge: Cambridge Univ. Press), 213
Zanda, B. 2004, Earth Planet. Sci. Lett., 224, 1
Zanda, B., Libourel, G., & Blanc, P. 2000, Meteorit. Planet. Sci., 35 Suppl., A176
Zanda, B., Libourel, G., & Blanc, P. 2005, Geochim. Cosmochim. Acta, submitted
Zieg, M. J., & Lofgren, G. E. 2002, Lunar Planet. Sci., 32, 1373
Zieg, M. J., & Lofgren, G. E. 2003, Lunar Planet. Sci., 34, 138